

# Temperature Rise Calculation and Optimization of Ceramic Sealed DC Contactor



Cong Qin , Xian Cheng , Guowei Ge , Qinglin Bai, and Shuai Du 

**Abstract** Aiming at the geometric model of 300 A DC contactor for electric vehicle and its charging pile, three-dimensional finite element electromagnetic field and steady-state thermal analysis simulation are carried out based on COMSOL. In the equivalent treatment of the heat source, the influence of the contact resistance in the contact system and the coil resistance in the electromagnetic system on the temperature rise is emphatically considered. In the simulation, the heat conduction inside the contactor and between the contactor and the connecting copper bar, the convective heat dissipation and radiation heat dissipation between the contactor and the external environment are considered, and the convective heat dissipation coefficient of each outer surface is calculated according to the thermal similarity theory. Using this model, the effects of the cross-sectional area of the connecting copper bar, the contact pressure between the contacts, the shell material, and the coil wire diameter on the temperature field distribution are studied, and the optimal design suggestions for improving the temperature rise characteristics are proposed, which can provide a reference for the miniaturization and large capacity design of the contactor.

**Keywords** Ceramic seal · DC contactor · Thermal analysis · Contact resistance · The optimization design

## 1 Introduction

Ceramic sealed DC contactors are widely used in new energy electric vehicles, charging piles, battery power supply, converter capacitor pre-charging, DC power control, circuit protection and other electric vehicles [1]. The contactor is the main component of the functional failure of the switching module. It is urgent to improve

---

C. Qin · X. Cheng · G. Ge (✉) · Q. Bai · S. Du  
School of Electrical Engineering, Zhengzhou University, Zhengzhou 450001, China  
e-mail: [ggw@zzu.edu.cn](mailto:ggw@zzu.edu.cn)

He'nan Engineering Research Center of Power Transmission and Distribution Equipment and Electrical Insulation, Zhengzhou 450001, China

© Beijing Paiké Culture Commu. Co., Ltd. 2024  
X. Dong and L. Cai (eds.), *The Proceedings of 2023 4th International Symposium on Insulation and Discharge Computation for Power Equipment (IDCOMPU2023)*, Lecture Notes in Electrical Engineering 1102, [https://doi.org/10.1007/978-981-99-7405-4\\_36](https://doi.org/10.1007/978-981-99-7405-4_36)

the performance and large capacity development of the required HVDC contactor [2]. The dynamic and static contacts of the ceramic contactor are sealed by special ceramics and filled with high-pressure arc extinguishing gas. Excessive temperature rise will lead to a decrease in mechanical strength and increase the contact resistance of the connecting part, further affecting the contact resistance and electrical performance of the contact. The contactor is developing towards miniaturization and large capacity, that is, it can withstand higher voltage and larger current loads without increasing the volume or even reducing the volume of the contactor [3]. This will lead to an increase in the load volume ratio of the contactor. Therefore, in order to ensure the long-term safe and reliable operation of the contactor, it is necessary to carry out thermal analysis.

Thermal analysis of power equipment is a complex problem involving the coupling of current field, gas field and temperature field [4]. A lot of research work has been done on electrical equipment. Polchow simulated the thermal field of the power connector, and considered the influence of the increase of contact resistance caused by wear on the temperature rise of the contact [5]. Barcikowski found that the influence of the internal convection and radiation heat transfer process on the steady-state temperature rise of the overall conductive circuit can be neglected [6]. Bo built a test platform for measuring the temperature rise characteristics of vacuum contactors. The temperature rise characteristics of the conductive circuit of the vacuum contactor contact system were simulated and compared with the test results [7]. Niu established the model to study the heat dissipation characteristics of the contactor and proposed a thermoelectric coupling calculation method to improve the calculation efficiency [8]. Luo conducted electro-magnetic thermal coupling simulation and experimental analysis on the temperature field of aviation variable frequency AC vacuum contactor [9]. Hu studied the influence of contact pressure, heat dissipation area, shell thickness and material, connecting rod material on the temperature field by changing different factors [10]. There are few literatures on the temperature rise characteristics of high-power DC contactors at home and abroad. The existing research is mainly focused on empirical formulas and electromagnetic mechanisms.

In this paper, the electromagnetic field simulation of the contactor is carried out based on the electromagnetic field theory, and the heating power of different components in the contactor is obtained. Based on the law of conservation of energy, the heat transfer differential equation is established to obtain the temperature distribution at different positions inside the contactor. By analyzing the influence of different factors on the temperature distribution, the structural design, material selection and parameter optimization of the product are guided to meet the requirements of miniaturization and large capacity.

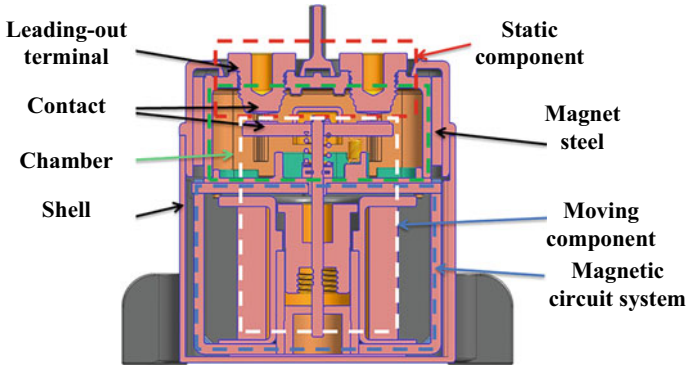


Fig. 1 Structure of the ceramic sealed DC contactor

## 2 Thermal Field Modeling and Parameter Calculation of Contactor

### 2.1 Research Object

The structure diagram of the research object is shown in Fig. 1, which is composed of magnetic circuit system, arc extinguishing chamber, contact and extraction end. The model is assumed as follows: The geometric features such as small fillets and screw holes in the model are ignored; the heating and heat transfer characteristics of small components such as spring system are ignored.

### 2.2 Heat Source Analysis and Parameter Calculation

In the simulation, the coil is equivalent to a hollow cylinder, as shown in Fig. 2.

The calculation formula of the equivalent heating rate of the coil resistance is:

$$q_v = \frac{P}{V} = \frac{U^2/R}{\pi(r_1^2 - r_2^2)h} \tag{1}$$

where  $q_v$  is equivalent heating rate,  $P$  is coil heat loss,  $V$  is coil volume,  $U$  is coil voltage,  $R$  is coil resistance,  $r_1$  is coil outer diameter,  $r_2$  is coil inner diameter,  $h$  is coil height.

The conductive bridge method is used to simulate the contact current shrinkage phenomenon in the electromagnetic analysis. In the thermal field analysis, the thin layer method is used to replace the contact resistance. The conductive bridge model and the thin layer model are shown in Fig. 3a, b.

The equivalent conductive radius of the conductive bridge is

**Fig. 2** Coil equivalent resistance model

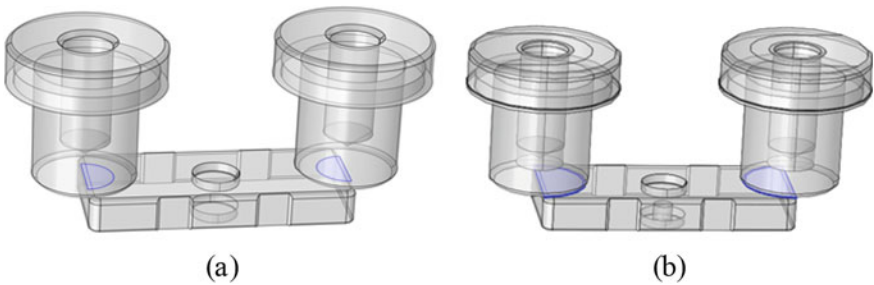
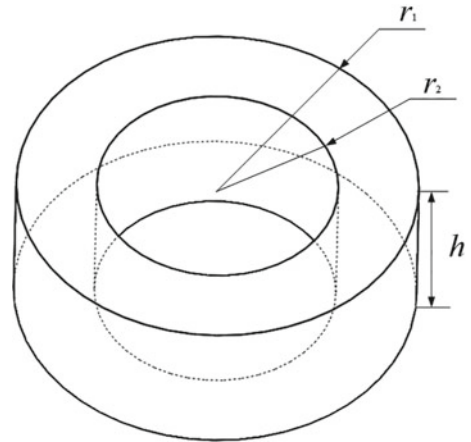


**Fig. 3** Conductive bridge model and contact thin layer model

$$r = \sqrt{\frac{F}{\pi \xi H}} \tag{2}$$

where  $F$  is the pre-pressure;  $\xi$  is a correction coefficient related to the contact condition of the contact surface, which ranges from 0.3 to 1.  $H$  is the Brinell hardness.

### 2.3 Heat Dissipation Characteristics Analysis and Parameter Calculation

The heat conduction satisfies the Fourier law:

$$q = -\lambda \frac{\partial T}{\partial n} \tag{3}$$

where  $q$  is the heat flux,  $\lambda$  is the thermal conductivity, and  $n$  is the length along the normal direction.

The thermal conductivity of the contact thin layer is obtained by Wiedemann–Franz formula:

$$\lambda = \frac{LT}{\rho} \tag{4}$$

where  $\lambda$  is the thermal conductivity of the contact thin layer,  $L$  is the Lorentz number,  $T$  is the absolute temperature,  $\rho$  is the resistivity of the contact thin layer.

The thermal convection inside and outside the contactor is natural convection. The basic formula of heat flow is Newton cooling formula:

$$q = h(T_w - T_f) \tag{5}$$

where  $h$  is the convective heat transfer coefficient,  $T_w$  is the wall temperature, and  $T_f$  is the fluid temperature.

For the contactor shell, the calculation formula is as follows:

$$\begin{cases} Gr = \frac{g\beta(t_w - t_f)l^3}{\nu^2} \\ Nu = f(Gr, Pr) = C(Gr Pr)^n \\ h = Nu \frac{\lambda}{l} \end{cases} \tag{6}$$

where  $Gr$  is the Grashev number;  $g$  is the acceleration of gravity;  $\beta$  is the bulk expansion coefficient;  $\nu$  is gas kinematic viscosity;  $l$  is the characteristic length;  $Nu$  is the Nusselt number;  $Pr$  is the Prandtl number;  $c$  and  $n$  are empirical constants.

Table 1 gives the selection basis of each parameter. On this basis, the convective heat dissipation coefficient of the surface of the contactor is calculated, as shown in Table 2.

The analysis of thermal convection inside the contactor belongs to the problem of natural convection heat dissipation in a limited space. For the vertical interlayer gas, when  $Gr \leq 2860$ , the heat transfer is completely dependent on heat conduction.

**Table 1** Selection of parameters for the calculation of convective heat dissipation coefficients

Surface shape	$Gr$	$C$	$n$	$L$
Cast or plate	$10^4-10^9$	0.59	1/4	Height
	$10^9-10^{11}$	0.10	1/3	
Plate, up	$2 \times 10^4-5 \times 10^6$	0.54	1/4	Rectangle: length; circle: diameter
	$5 \times 10^6-10^{11}$	0.15	1/3	
Plate, down	$3 \times 10^5-3 \times 10^{10}$	0.27	1/4	

**Table 2** Anisotropic convective heat dissipation coefficient of contactor outer surface

Contactor surface in all directions	Heat convection coefficient ( $\text{W m}^{-2} \text{K}^{-1}$ )
Flank	5.00
Top surface	5.90
Bottom surface	2.95

$$G_{r\delta} = \frac{g\beta\Delta T\delta^3}{v^2} \tag{7}$$

The maximum thickness of the internal gas in this model is 13 mm. When the outer wall temperature is 57.1 °C, the  $G_{r\delta}$  is 2340, so only heat conduction can be considered.

The radiation energy can be obtained by Stefan-Boltzmann law:

$$E = \varepsilon\sigma(T^4 - T_0^4) \tag{8}$$

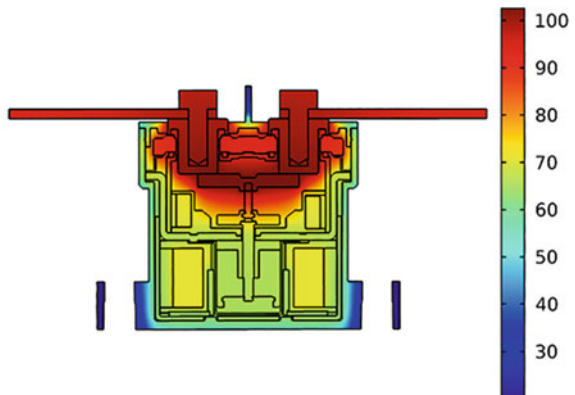
where  $E$  is the radiation energy,  $\varepsilon$  is the emissivity,  $\sigma$  is the blackbody radiation constant,  $T^4$  is the surface temperature and  $T_0^4$  is the ambient temperature.

The radiation emissivity of the shell is set to 0.90, and the copper part is set to 0.22.

### 3 Thermal Analysis Results

Firstly, the current density distribution is calculated by the AC / DC module, and then the corresponding heating power of each conductor is calculated. The temperature distribution of the contactor section is shown in Fig. 4.

**Fig. 4** Temperature distribution at the center interface of the DC contactor



The highest temperature of the contactor with connecting line appears near the main contact, which is 78.15 °C, and the temperature of the terminal is 75.8 °C, which meets the requirements of the national standard. In the temperature rise test, the temperature rise at the terminal is 50.1 °C, while the simulated temperature rise is 48.8 °C, and the error is only 2.6%. The model can be used for the analysis of the influencing factors of temperature field. Analysis of influencing factors of temperature field.

### 3.1 External Factors

The terminal is fixed by a screw to connect the copper plate to the power supply. The copper plate will take away a certain amount of heat through heat conduction and heat convection. The influence of copper plate must be considered. The cross-sectional area in the initial model is 35 mm<sup>2</sup>, and the contact temperature rise is 49.2 °C. When the cross-sectional area increases by 47%, the temperature rise decreases by 8.0 °C. When the cross-sectional area increases, not only the heat conduction effect of the main circuit will be enhanced, but also the overall heat dissipation area will increase, which enhances thermal convection and thermal radiation (Fig. 5).

**Fig. 5** Relationship between contact temperature and cross-sectional area of copper plate

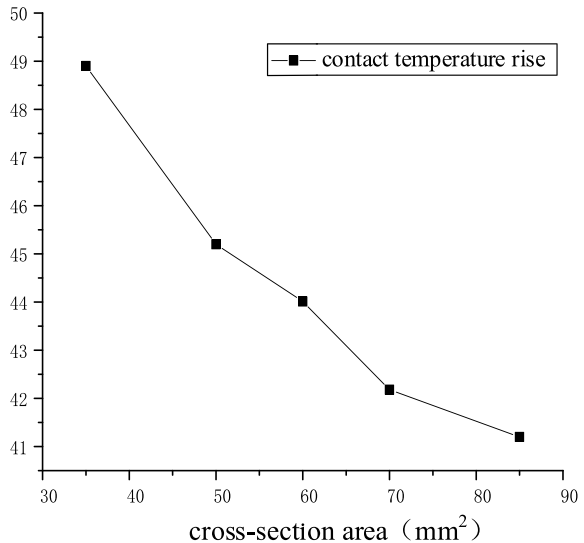
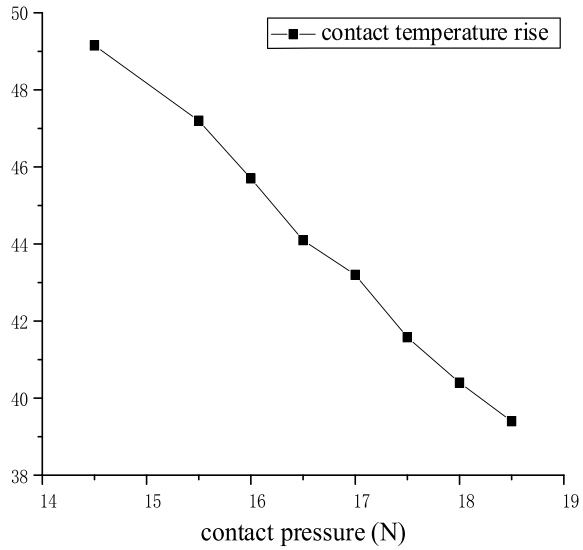


**Fig. 6** Relation between contact temperature rise and contact pressure



### 3.2 Internal Factors

The contact pressure in-creases by 4 N, and the temperature rise of the contact de-creases by 16.6 °C. This is because the contact pressure between the contacts is an important factor affecting the contact resistance, and the greater the contact pressure, the smaller the contact resistance (Fig. 6).

The property of the shell is one of the important factors. The conductivity of the original contactor is 0.24 W m<sup>-1</sup> K<sup>-1</sup>. After changing the BMC with a thermal conductivity of 3.0 W m<sup>-1</sup> K<sup>-1</sup>, the temperature rise of each key point is shown in Fig. 7. The shell material with better thermal conductivity can significantly reduce the temperature of the contacts and coils, but the temperature of the shell will increase.

The empirical formula of the thermal conductivity of the coil is:

$$\lambda = \sqrt{a\lambda_1\lambda_0(d_1/d_2 - 1)} - b\lambda_0 \tag{9}$$

where *a* and *b* are 1.45 and 1.6, λ<sub>1</sub> is the conductivity of the insulation, λ<sub>0</sub> is the conductivity of the air, *d*<sub>1</sub> is the diameter of the wire, and *d*<sub>2</sub> is the insulation thickness (Table 3).

The larger the coil diameter, the lower the coil temperature rise. Increasing the wire diameter reduces the thermal conductivity of the coil and enhances the heat transfer effect; without changing the number of ampere turns, the larger the wire diameter of the coil, the smaller the resistance value, the smaller the heat loss, and the smaller the temperature rise.

The following is the temperature rise of each key component before and after optimization (Fig. 8).



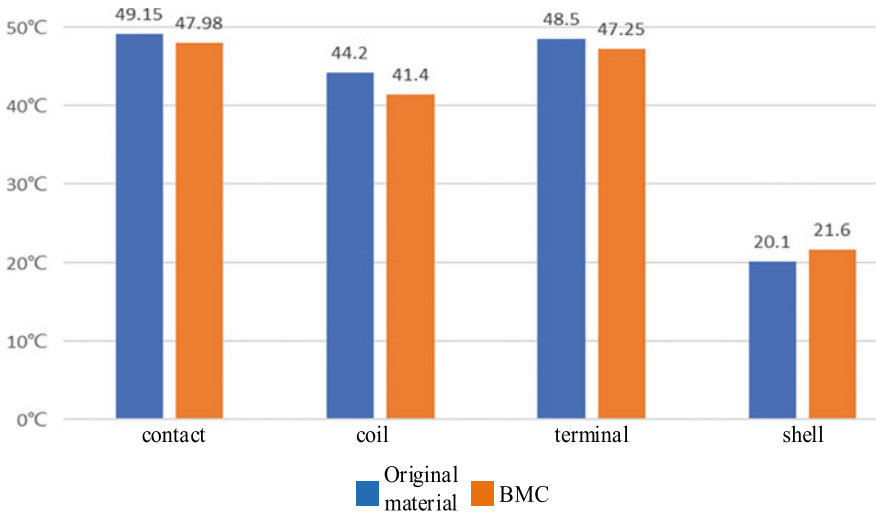


Fig. 7 Temperature rise of key parts after changing shell material

Table 3 Simulation values of thermal conductivity and coil internal temperature rise

Diameter of wire $d_1$ (mm)	Insulation thickness $d_2$ (mm)	Thermal conductivity $\lambda$ (W/(m K))	Maximum scale temperature-rise (°C)
0.5	0.025	0.312	44.2
0.55	0.025	0.331	40.6
0.6	0.025	0.348	31.6

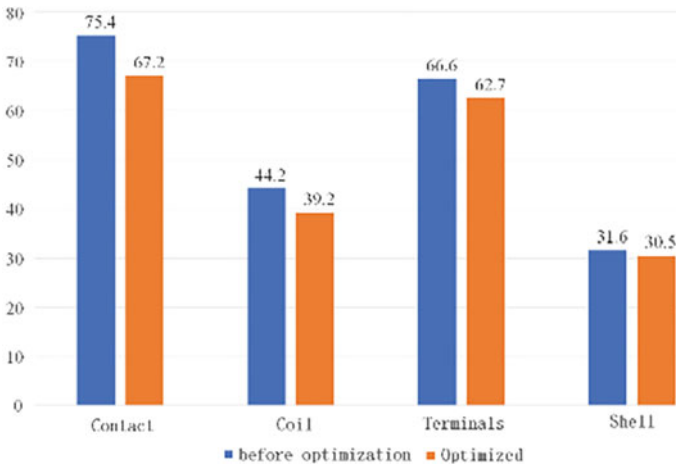


Fig. 8 Temperature rise of key components before and after optimization

The temperature rise of each key component decreases after optimization, and the temperature rise of the contact decreases the most, which is 8.2 °C. The effectiveness of the above optimization measures is proved. From the perspective of the temperature rise of long-term stable operation, without changing the structure and without increasing its volume, these optimization measures can be taken to improve the current level and make it withstand a larger capacity load.

## 4 Conclusions

- (1) The influence of the cross-sectional area of the connecting copper plate on the temperature field is analyzed. With the increase of the cross-sectional area of the connecting copper plate, the temperature rise of the contact will decrease.
- (2) The influence of the temperature field distribution of the contact pressure contactor is analyzed. When the contact pressure increases by 4 N, the temperature rise of the contact decreases by 16.6 °C. That increasing the contact pressure of the contact can reduce the contact resistance, thereby reducing the temperature rise of the contact.
- (3) The influence of shell material on the temperature field distribution of contactor is analyzed. The shell material with stronger thermal conductivity can reduce the temperature rise of each key part.
- (4) The influence of the coil diameter is analyzed without changing the number of coil ampere turns. The increase of coil diameter is beneficial to the decrease of temperature rise from both heating and heat dissipation characteristics.

## References

1. Subramaniam K (2020) Intelligent three tie contactor switch unit-based fault detection and isolation in DC microgrids. *IEEE Trans Ind Appl* 56(1):95–105
2. Gonzalez D (2020) Switching behavior of a gas-filled model DC-contactor under different conditions. *IEEE Trans Plasma Sci* 48(7):2515–2522
3. Ghassemi M (2015) A coupled computational fluid dynamics and heat transfer model for accurate estimation of temperature increase of an ice-covered FRP live-line tool. *IEEE Trans Dielectr Electr Insul* 21(6):2628–2633
4. Mohsin L (2014) Finite element analysis of stress intensity factor of pre-cracked coated substrate under contact sliding. In: *Electronics 2014 IEEE 36th international conference on manufacturing technology*, pp 1–4
5. Polchow JR (2010) A multi-physics finite element analysis of round pin high power connectors. In: *Proceedings of the 56th IEEE holm conference on electrical contacts and the 25th international conference on electrical contacts*, pp 30–38
6. B.F. (2000) Simulations of the heat balance in low-voltage switchgear. In: *Proceedings of 20th international conference on electrical contacts*, pp 322–329
7. Luo X (2021) Study on thermal characteristics of aviation frequency AC vacuum contactor based on electromagnetic-thermal coupling. *Vacuum Electron* 353(04):57–63 (in Chinese)

8. Niu C (2021) Thermal dissipation characteristics analysis and coupling iterative thermal analysis method of aviation contactor. *High Volt Eng* 47(02):487–494 (in Chinese)
9. Bo K (2019) Experiments and simulation analysis of the temperature-rise characteristics of high current vacuum contactor. *Trans China Electrotech Soc* 34(24):5135–5143 (in Chinese)
10. Zhang X (2019) Discussion on the lectotype design of high voltage distribution box for electric vehicles. *Popul Sci Technol* 21(12):42–43+41 (in Chinese)